tvst

https://doi.org/10.1167/tvst.8.4.3

Article

Leber's Hereditary Optic Neuropathy–Specific Heteroplasmic Mutation m.14495A>G Found in a Chinese Family

Shouqing Li[1], Shan Duan[2,3], Yueyuan Qin[2,3], Sheng Lin[2,3], Kaifeng Zheng[2,3], Xi Li[2,3], Linghua Zhang[2], Xueying Gu[2], Keqin Yao[2], and Baojiang Wang[2,3]

[1] Department of Neuro-ophthalmology, Weifang Eye Hospital, Shandong Province, China
[2] Laboratory of Medical Genetics, Shenzhen Health Development Research Center, Shenzhen, China
[3] Center for Birth Defect Research and Prevention, Shenzhen Health Development Research Center, Shenzhen, China

Correspondence: Baojiang Wang, Laboratory of Medical Genetics, Shenzhen Health Development Research Center, no. 4009 Xinzhou Road, Futian District, Shenzhen City 518040, China. e-mail: wangcell@163.com

Received: 1 October 2018
Accepted: 6 May 2019
Published: 3 July 2019

Keywords: LHON; m.14495A>G; heteroplasmy; mtDNA copy number; dPCR

Citation: Li S, Duan S, Qin Y, Lin S, Zheng K, Li X, Zhang L, Gu X, Yao K, Wang B. Leber's hereditary optic neuropathy–specific heteroplasmic mutation m.14495A>G found in a Chinese family. Trans Vis Sci Tech. 2019;8(4):3, https://doi.org/10.1167/tvst.8.4.3

Purpose: Leber's hereditary optic neuropathy (LHON) is a mitochondrial DNA (mtDNA)-associated, maternally inherited eye disease. Mutation heteroplasmy level is one of the leading causes to trigger LHON manifestation. In this study, we aimed to identify the causative mutation in a large Han Chinese family with LHON and explore the underlying pathogenic mechanism in this LHON family.

Methods: The whole-mtDNA sequence was amplified by long-range PCR. Mutations were subsequently identified by next-generation sequencing (NGS) and validated by Sanger sequencing. The heteroplasmy rates of those family members were determined by digital PCR (dPCR). Mitochondrial haplogroups were assigned based on mtDNA tree build 17.

Results: The m.14495A>G mutation was identified as causative due to its higher heteroplasmy level (>50%) in patients than in their unaffected relatives. All mutation carriers belong to M7b1a1 and are assigned to Asian mtDNA lineage. Interestingly, our result revealed that high mtDNA copy number in carrier might prevent LHON manifestation.

Conclusions: This is the first report of m.14495A>G mutation in Asian individuals with LHON. Our study shows that dPCR technology can provide more reliable results in mutation heteroplasmy assay and determination of the cellular mtDNA content, making it a potentially promising tool for clinical precise diagnosis of LHON. Furthermore, our results also add evidence to the opinion that higher mtDNA content may protect mutation carriers from LHON.

Translational Relevance: dPCR can be used for the assessment of LHON disease, and a new genetic-based diagnostic strategy has been proposed for LHON patients with the m.14495A>G mutation.

Introduction

Leber's hereditary optic neuropathy (LHON) is one of the most common mitochondrial DNA (mtDNA) diseases, which is characterized by acute or subacute bilateral central vision loss due to selective death of retinal ganglion cells (RGCs) and optic atrophy.[1–3] The disease is typically detected in young adults and more frequently affects males, predominantly.[4] Point mutation of mtDNA is the major cause of the disease,[5] and the following three-point mutations, m.3460G>A in *MT-ND1*, m.11778G>A in *MT-ND4*, and m.14484T>C in *MT-ND6*, have been found in over 90% of LHON population.[6]

Currently, the diversity is presented in the mechanisms for triggering the clinical manifestation of LHON. First, harboring a primary mutation is the main way of causing LHON. However, not all carriers would become affected.[7,8] Only approximate-

ly 50% of the males and 10% of the females carrying a primary mutation eventually could manifest visual symptoms.[9] Such incomplete penetrance is an unexplained issue to date for LHON disease,[3] suggesting additional factors, such as mtDNA background, nuclear background, and environment factors, might contribute to the disease expression.[10–14] Second, secondary mtDNA mutation could act synergistically with the primary mutation to modulate the LHON expression. For instance, two secondary mutations, m.4216T>C and m.13708G>A, which co-occurred with primary mutation m.11778G>A on haplogroup J were reported to increase the penetrance of LHON.[15] And another secondary mutation, m.14502T>C interacting with primary mutation m.11778G>A can result in a further reduction of complex I activity and thereby more severe symptoms.[16] Third, heteroplasmic load of mutation (% of mutated mtDNA) can also affect the disease expression. It was reported that approximately 10% to 15% of LHON mutation carriers are heteroplasmic (a mixture of mutated and wild-type mtDNA),[17,18] and a hetroplasmic load of at least 60% is required for clinical manifestations of LHON.[18,19] A newly published study reported a LHON case with the heteroplasmic mutation, m.13094T>C, in which patient showed a rapid visual recovery accompanied by a decrease of the percentage of mutant mtDNA.[20]

Here, a known LHON-associated point mutation (m.14495A>G) was identified and evaluated in a Han Chinese family. Its heteroplasmic level was determined by using digital PCR (dPCR) technology due to the inability of real-time PCR for this mutation. We also evaluated the contribution of heteroplasmy to the manifestation of LHON disease in this family and proposed a reference value of mutational load for m.14495A>G that may benefit LHON diagnosis.

Material and Methods

Patients

A Han Chinese, six-generation family with LHON was recruited from the Department of Neuro-ophthalmology at Weifang Eye Hospital, Shandong Province. All patients provided informed consent. The study was approved by the Shenzhen Health Development Research Center Review Board and carried out in accordance with the Declaration of Helsinki. The clinical phenotypes were determined by ophthalmologic examinations. Blood samples were collected from 17 members indicated in Figure 1. The 63 family members are composed of 18 affected and 45 unaffected subjects, including 37 carriers who's mutant mtDNA follow the maternal inheritance.

Mutational Analysis of mtDNA

Genomic DNA was extracted from peripheral blood using the NucleoSpin Blood Kit (Macherey-Nagel, Duren, Germany). The entire mtDNA sequence was amplified in three overlapping fragments using long-range PCR with the following primers: 5′-CCCACTCCCATACTACTAATCTCATC-3′/ 5′-TAAGGAGAAGATGGTTAGGTCTACGG-3′ (amplified region 463-6354), 5′- GAGCCTTCAAAGCCCTCAGTAA-3′/ 5′-CGAACAATGCTACAGGGATGAAT-3′ (5539-12623), and 5′-CTATAACCACCCTAACCCTGACTTC-3′/ 5′-TCAGTGTATTGCTTTGAGGAGGTAAG-3′ (12354-614). PCR was performed at 94°C for 1 minute, followed by 30 cycles (10 seconds at 98°C, 30 seconds at 65°C, and 10 minutes at 68°C), and a final extension for 10 minutes at 68°C. The resulting PCR products were fragmented and labeled with barcodes to indicate their sample origin. Electrophoresis was performed to isolate that 250 to 300 bp of DNA fragments and these obtained fragments were subsequently amplified by using different barcoded primers for each library. Then barcoded libraries were pooled, purified, and sequenced on the Ion PGM sequencing platform (IonTorrent; ThermoFisher Scientific, Waltham, MA) according to manufacturer's instructions. A mean sequencing depth of more than 1000× was achieved. Data analysis was performed and Mitomap (www.mitomap.org/MITOMAP) and mtDB (www.mtdb.igp.uu.se/) were used as reference database. All the mutations were compared with the revised Cambridge Reference Sequence (rCRS; NC_01290) and were finally validated by Sanger sequencing.

Nd6 Protein Sequence Alignment

ND6 protein sequences were extracted from the National Center for Biotechnology Information Homologene database and aligned using DNAMAN software (version 7) across 15 species, including mammals, reptiles, amphibians, birds, fish, and insects.

Mitochondrial DNA Complete Sequencing and Phylogenetic Analysis

Sanger sequencing of entire mtDNAs was performed in 24 overlapping fragments using 24 sets of

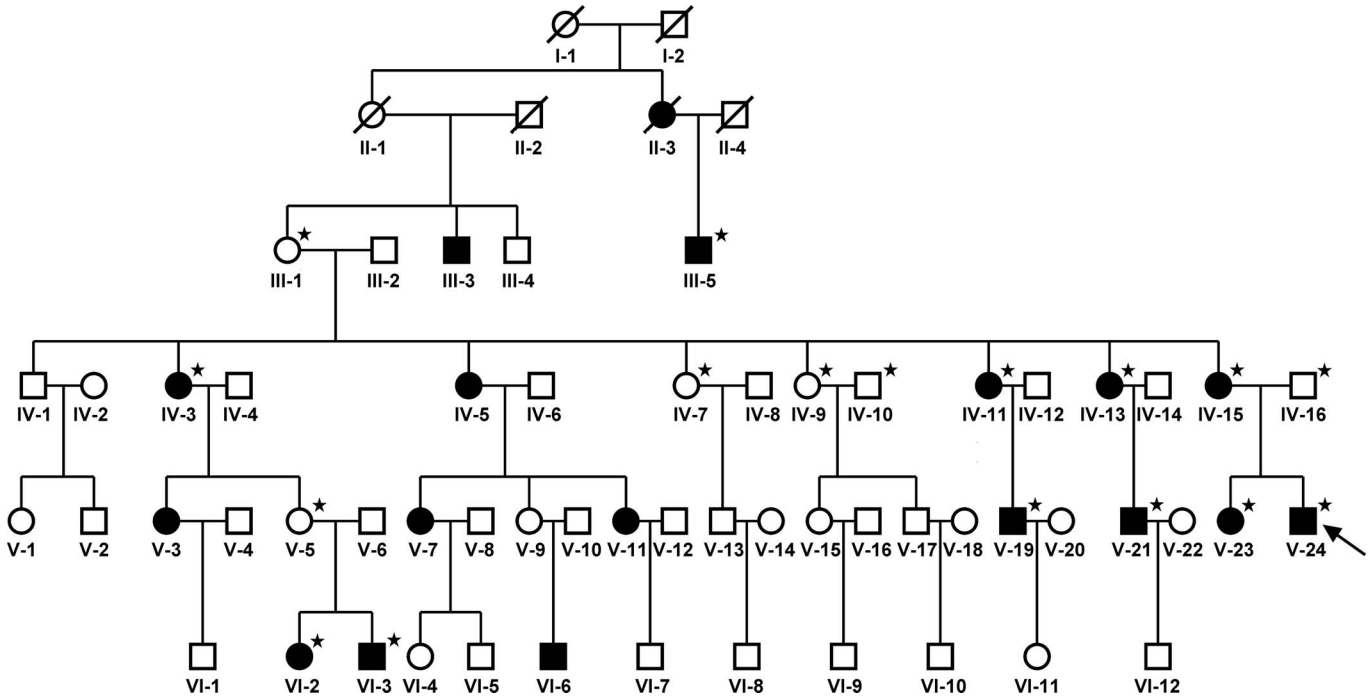

Figure 1. Pedigree of the LHON family. Family members whose blood samples were collected are marked with an *asterisk* and the proband is indicated by a *black arrow*. Vision impaired individuals are indicated by *filled symbols*.

primers as described previously.[21] Complete mtDNA sequences of family members have been deposited in GenBank database with the following accession numbers: MH973718 and MH973719. They were then submitted to the https://haplogrep.uibk.ac.at/ for phylogeny construction.

Preparation of Vector Containing m. 14495A>G mutation

DNA from family members (IV-7 and V-21) was amplified using the primers 5′- CCCATCA-TACTCTTTCACCCA-3′ and 5′- CCAAGGAGT-GAGCCGAAGT-3′ (amplified region 14341-14859), respectively. The resulting 519-bp product was purified and cloned into the pGEM-T Easy Vector (Promega, Madison, WI). Two clones were selected for serving as positive templates as follows: one harboring 14495A (wild type) and the other harboring 14495G (mutant). They could be used as calibrants to evaluate the reliability of quantitative assay.

Quantification Using Real-Time Quantitative PCR

A total of 20 μL of PCR reaction was prepared according to manufacturer's protocols, containing 0.2 μM of each primer, 0.2 μM of each Taqman-MGB probe, and serial dilutions of the DNA samples. Taqman-MGB probes were designed to target the m.14495A>G mutation, with VIC label for wild-type allele and FAM for mutant one (primers and probes sequence information available upon request). Real-time PCR assays were performed in LightCycler 96 System (Roche Diagnostics, Mannheim, Germany) with the following PCR conditions: 30 seconds at 95°C, 40 cycles at 95°C for 10 seconds, and at 60°C for 30 seconds and a final cooling at 50°C for 30 seconds. Experiments were performed three times for all the samples.

Quantification Using Digital PCR

A total volume of 15 μL of dPCR reaction was prepared, containing 1× QuantStudio Three-Dimensional (3D) Digital Master Mix v2 (Life Technologies, Frederick, MD), 0.4 μM of each primer, 0.2 μM of each Taqman-MGB probe, and 93.33 pg of genomic DNA equivalent to 28 genomic DNA copies. Then, 14.5 μL of PCR reaction was loaded onto a QuantStudio 3D v2 dPCR chip (Life Technologies, Pleasanton, CA) and amplification was performed in a ProFlex 2× flat block thermal cycler (Life Technologies, Carlsbad, CA) following a recommended amplifying method from manufacturer's protocol. After imaging the chip using the QuantStudio 3D

Chip-Reader (Life Technologies), the data were analyzed by using the QuantStudio 3D Analysis Suite Cloud Software.

mtDNA Copy Number

In general, 50-ng human DNA is approximately equal to 15,000 copies of human genomic DNA according to the manual of 3D digital PCR. We all know that each cell contains two copies of genomic DNA, namely two genomic DNA molecules equivalent to one cell. In this study, we guaranteed to load absolutely equal amount of genomic DNA to each 3D Digital PCR chip. Thus, mtDNA copy number per cell could be calculated on the base of dPCR results in combination with the above parameters.

Statistical Analysis

Statistical analyses were performed using the Mann-Whitney U test. Statistical significance was set at $P < 0.05$.

Results

Clinical Features of LHON Family

The family originated from the city of Zhucheng in Shandong Province of China. The proband was a 14-year-old boy suffered from sudden progressive deterioration of vision in the right eye and the same symptom appeared in the left eye after 1 week. His vision declined rapidly with best-corrected visual acuity (BCVA) falling to the level of finger counting (CF/10 cm) in both eyes. Fundus examination showed optic disc hyperemia with telangiectatic vessels (Fig. 2A). Visual field analysis revealed dense visual field defects connected to the physiological blind spot in the right eye. Seven months later, the symptom developed further into a binocular optic pallor (Fig. 2B), whereas the corneas of both eyes remained transparent and the pupils responded well to light. Optical coherence tomography (OCT) examination showed that the peripapillary retinal nerve fiber layer (RNFL) became thinner in both eyes, but no abnormal symptoms appeared in other body parts. The patient was routinely treated with nerve nutrition agent and functional drug that improves blood circulation. One year later, the BCVA was 0.05 in both eyes, suggesting the progressive improvement in visual function and the BCVA of both eyes could be restored to 0.8 in the following year. His 21-year-old sister and 45-year-

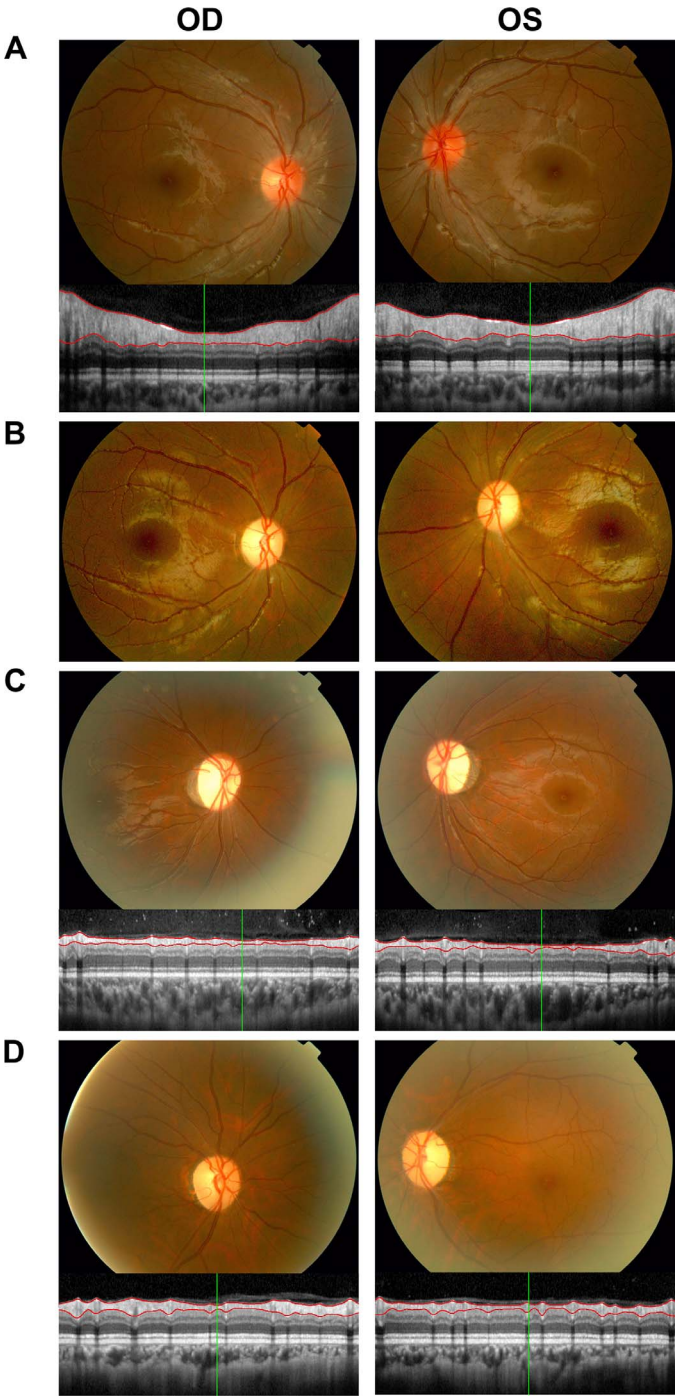

Figure 2. Ophthalmic images of patients with LHON. (A) Patient V-24 manifested as optic disc hyperemia with telangiectatic vessels. (B) Patient V-24 further developed a binocular optic pallor or atrophy, but the main direction of vessels is normal. (C) Patient V-23 exhibited optic atrophy with narrowing vessels. (D) Patient IV-15 exhibited diffused atrophy of the optic disc in both eyes. The accompanying OTC images were presented underneath fundus photographs, showing a significant reduction in RNFL thickness, especially in patients V-23 and IV-15.

old mother were also involved in the similar clinical problems (Figs. 2C, 2D). Overall, patients in this family presented typical LHON features, including severe visual impairment, bilateral optic disc pallor, and narrowed vessels, which finally led to optic atrophy (Fig. 2). By combining the fact of a clear maternal family history, we concluded that this family was subject to a LHON disease.

Screening of LHON Mutations

Forty-six variants were identified, 14 of which are harbored at noncoding region of mitochondrial genome, and were negative for three most common point mutations. A total of 12 variants were present as nonsynonymous (Supplementary Table S1), of which three, m.4136A>G (p.Y277C) in *MT-ND1*, m.14495A>G (p.L60S) in *MT-ND6*, and m.15257G>A (p.D171N) in *MT-CYB*, are private mutations of this family and they previously were reported to be associated with LHON. m.4136A>G that causes a tyrosine to cysteine amino acid substitution in *MT-ND1* was initially reported as pathogenic in a Queensland LHON family,[22] whereas with a low pathogenicity score of 0.374.[23] The frequency data derived from MITOMAP database, show a frequency of more than 1% (1.08%) in M7b haplogroup, suggesting that it plays a role of polymorphism. m.15257G>A was reported to be associated with 9% of LHON cases,[24] but some controversies exist with respect to its pathogenic power. It either appears alone or in combination with a primary mutation like m.11778G>A and m.14484T>C, respectively, suggesting it more likely to act as an intermediate mutation.[25] A subsequent study characterized it as a marker of J subclades and classified as a benign variant.[26] Most importantly for both m.4136A>G and m. 15257G>A, they present consistent heteroplasmic level between affected and unaffected individuals according to the ratio of mutant reads obtained from next-generation sequencing (NGS) data analysis (Supplementary Table S1), indicating that these two mutations are unlikely to be pathogenic in this family. In contrast, the m.14495A>G mutation presents altering of heteroplasmy with LHON manifestation (Supplementary Table S1) and showing much higher heteroplasmic level in affected than in unaffected individuals. Thus, m.14495A>G mutation was more likely to be considered as a causative factor for this LHON family. However, NGS used to quantify the heteroplasmic load might not be a very accurate approach because of the introduction of amplification bias during the long-range PCR that was produced prior to sequencing.

Characteristics of m.14495A>G

m.14495A>G was first discovered in 2001, in a British and a Canadian LHON family, which belong to haplogroup H,[27] but lack enough evidence to confirm its pathogenicity. Mitchell et al.[5] subsequently developed a scoring system defining the mutation as possibly pathogenic. In this system, they also assess the mutation m.4136A>G a neutral sequence variant, namely polymorphism. The third appearance of m.14495A>G is in an Italian family as a primary mutation.[26] It should be noted that its segregating in our LHON family further indicated that m.14495A>G should be pathogenic. In addition, protein sequence alignment showed that the corresponding amino acid residue is evolutionarily conserved among a wide range of species (Supplementary Fig. S1). The resulting missense mutation causes the replacement of nonpolar leucine with a polar serine, which was predicted to change the hydrophobicity profile of ND6 protein.

Haplogroup Distribution Among Family Members

The mtDNA haplogroup was assigned based on the mutations in the mtDNA complete sequences of family members. All maternally related individual in this family belonged to the haplogroup M7b1a1 + (16192), whereas the remaining two individuals, IV-10 and IV-16, belonged to haplogroup B4d3 (Fig. 3). We also found that some family members, such as III-1, IV-3, IV-7, and IV-9, harbored the m.11257 mutation in a heterozygous status, but this mutation does not change the protein function due its synonymous substitution.

Assay Evaluation Between Real-time PCR and dPCR

Urata et al.[28] demonstrated that a mutational load as low as 0.1% can be clinically significant. Therefore, particular attention should be given to the accuracy of the quantification. In order to achieve that, the reliability between real-time PCR and dPCR technology was first compared by using linear regression analysis for a serial of DNA mixtures at different mixing ratios of wild-type and mutated plasmids. These constructed mixtures were used to represent the range of mutation loads from 0% to 100%. According to the calibration curves generated

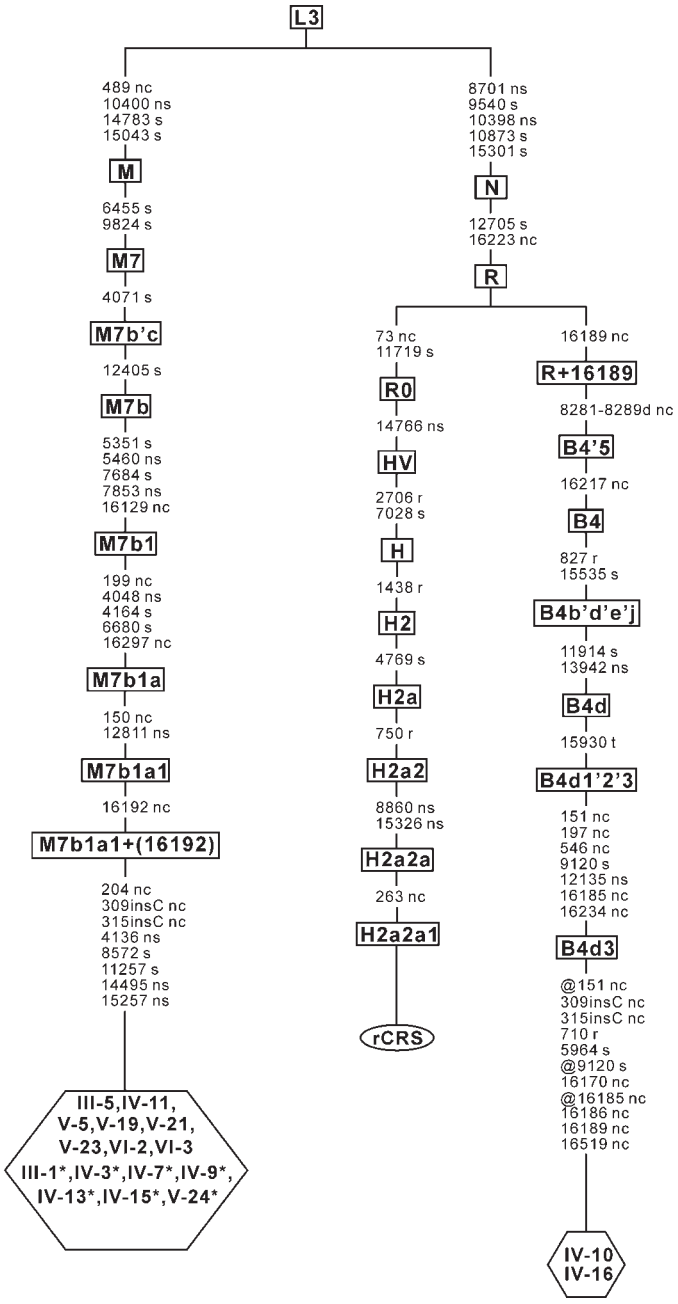

Figure 3. The phylogenetic tree of LHON family members. The synonymous and nonsynonymous coding-region variants are denoted by 's' and 'ns', respectively. Variants in the transfer RNA and the ribosomal RNA genes are denoted by 't' and 'r', respectively. The insertions, deletions, and noncoding variants are denoted by 'ins', 'd', and 'nc', respectively. Assumed back mutations are indicated with a '@' prefix. Family members whose mtDNA mutations, both m.11257C>T and m.14495A>G, present in heteroplasmic state documented by using Sanger sequencing were marked by *star*.

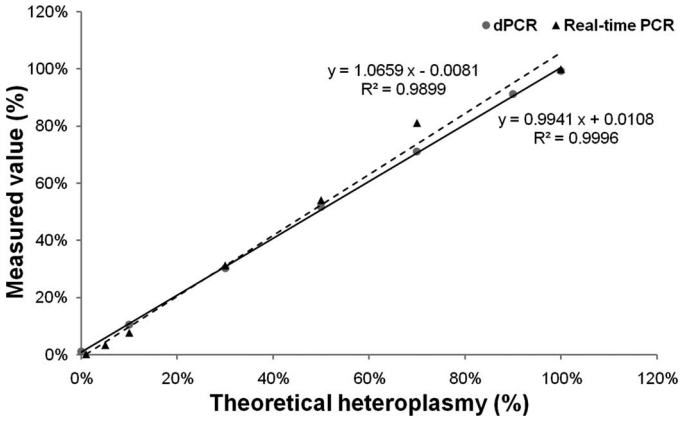

Figure 4. Standard curves from cloned wild-type and mutated DNA samples, which have been mixed at various mutation loads ranging from 1% to 100%. Standard curve showing a linear relationship between input and detected values of the heteroplasmy were created based on the quantification results from Real-time PCR (*dotted line*) and dPCR (*solid line*). Slope and R^2 was determined by using linear regression analysis.

from 0.00001 to 0.1 ng of plasmid DNA by real-time PCR (data not shown), we obtained the absolute concentration of each plasmid component in 1 pg of mixtures and thereby could figure out their mutation load (Fig. 4). For dPCR, 0.0451 pg of plasmid mixture with different mutation loads was also quantified. As shown in Figure 4, dPCR is more reliable than real-time PCR, because the correlation coefficient ($R^2 = 0.9996$) is higher and the slope is much closer to 1.

Heteroplasmy of m.14495A>G

Estimation of heteroplasmy of m.14495A>G in the LHON family was performed by using dPCR system. In order to ensure the equal amount of DNA was loaded onto the 3D digital PCR chip, quantification of each DNA sample was performed in triplicates by using Qubit 2.0 Fluorometer (Life Technologies) and took the average. As shown in the Table, patients present higher levels of heteroplasmy, which are above 50%. We found that patients would develop LHON at a younger age as heteroplasmy level increased and the correlation is statistically significant (Spearman's $r = -0.819$, $P = 0.002$). We also noted that real-time PCR technology did encounter some drawbacks and problems. It fails to detect the wild-type allele in carriers whose heteroplasmy rate was greater than 90%. Instead, a heteroplasmy of 100% was usually obtained for them (Table), indicating a relatively low sensitivity to m.14495A genotype in the use of real-time PCR for

Table. Heteroplasmy Rate of m.14495A>G Mutation and Cellular mtDNA Content of All Available Family Members

Subject ID	Sex	Age at Onset, y	Heteroplasmy, %				mtDNA Copy Number/Cell	
			NGS Value	Real-Time PCR Value	dPCR		dPCR	
					Value	95% CI	Value	95% CI
III-5*	M	12	99.20	100.00	96.93	90.65–103.56	172.25	161.21–184.18
IV-3*	F	19	74.53	69.94 ± 1.70	66.07	61.56–70.86	185.53	172.98–199.14
IV-11*	F	15	98.01	100.00	96.98	90.15–104.25	143.83	133.80–154.73
IV-13*	F	17	88.97	93.31 ± 1.16	89.35	82.12–97.14	109.88	101.06–119.56
IV-15*	F	16	89.03	88.07 ± 2.61	86.11	79.42–93.29	125.83	116.15–136.43
V-19*	M	10	97.97	100.00	99.70	91.94–108.03	114.74	105.89–124.42
V-21*	M	13	93.33	100.00	98.04	91.62–104.84	167.54	156.68–179.29
V-23*	F	13	98.25	100.00	99.88	93.95–106.11	198.05	186.43–210.55
V-24*	M	16	92.64	100.00	94.88	88.44–101.72	161.58	150.72–173.35
VI-2*	F	11	100.00	100.00	99.58	92.95–106.62	152.20	142.15–163.07
VI-3*	M	12	98.32	100.00	99.36	92.84–106.25	165.08	154.37–176.66
III-1	F	-	28.07	19.21 ± 1.59	24.27	21.83–26.95	154.71	139.30–171.98
IV-7	F	-	61.36	45.05 ± 4.28	39.78	35.31–44.77	81.50	72.41–91.81
IV-9	F	-	47.50	26.95 ± 0.87	32.38	29.61–35.38	193.56	177.16–211.68
V-5	F	-	99.12	100.00	98.45	93.74–103.32	392.96	374.43–412.72
IV-10	M	-	0.00	0.00	0.00	NA	138.57	NA
IV-16	M	-	0.00	0.00	0.05	0.0095–0.31	141.05	131.57–151.30

F, female; M, male; CI, confidence interval; NA, not available.
* Represent patients in the family.

the detection of heteroplasmy of m.14495A>G. The flanking sequence adjacent to position m.14495 contains highly repetitive C and A (Supplementary Fig. S1), inevitably resulting in a reduction of the probe specificity. However, dPCR technology can overcome such embarrassment by allowing merely a single copy of DNA molecule into each well of chip and achieve an attempt to reduce the complexity of templates and thereby increase the sensitivity to targeted DNA molecules. Herein, dPCR is experimentally validated for reliable use in determining DNA copy number with accuracy within 5% of expected values (Supplementary Table S2), which fully meets the requirements for quantitative analysis. We also noted that the calls of different genotypes in the scatter plot view are clearly separated (Supplementary Fig. S2), and more accurate heteroplasmic values could be observed among family members (Table). Attractively, V-5 had a high-mutation heteroplasmy (>98%) but did not develop the disease possibly because the high mtDNA content compensated for the defects of the m.14495A>G mutation.

Discussion

The study on heteroplasmy in LHON has long been a hot topic.[20,29,30] Retinal ganglion cells (RGCs) are one of the most important targeting tissues of LHON,[19] but they are inaccessible for genetic test. Thus, we then asked whether mtDNA assessment in peripheral blood cells could reflect the heteroplasmic load in RGCs. Bianco et al.[31] investigated the heteroplasmy of the primary mutation m.3460G>A in peripheral blood cells. They found that there were subjects with heteroplasmy of 100% or 15% to manifest LHON symptoms, while some subjects with heteroplasmy ranging from 55% to 75% exhibited without LHON, indicating no correlation between the clinical expression of LHON and heteroplasmic load of mutation. However, in our study, the heteroplasmy level of m.14495A>G was significantly different between affected and unaffected mutation carriers ($P < 0.01$, Supplementary Fig. S3A). This suggests that high-heteroplasmy level for the m.14495A>G mutation is a crucial factor in LHON pathogenesis and its value over 60% in the peripheral blood is a risk signal for the development of LHON. In addition,

patients in our study remain asymptomatic except visual loss. Because RGCs are the most common LHON affected cells, the reduction of mutation load in the blood is likely to be accompanied by a decrease in the RGCs mutation load. Our result is in line with the threshold value of 60% proposed previously in a study involving 17 families.[18] As a more secure strategy for LHON prevention, we propose here that heteroplasmy of less than 50% for m.14495A>G is considered to be safe. In summary, the heteroplasmy threshold required for LHON manifestation may be variable for different mutations.

Mitochondrial DNA haplotype was also reported to influence the clinical expression of LHON. In western European, the J2 and J1 haplogroups have been reported to contribute to increased risk of visual failure in families with m.11778G>A and m.3460G>A mutations, respectively.[10] An investigation in Chinese population showed that haplogroups M7b and M10a increased penetrance in individuals with m.11778G>A, whereas haplogroup F might confer a protective effect against LHON.[32] Achilli et al.[26] reported an Italy family with m.14495A>G mutation in the H66 haplogroup,[26] and the penetrance was calculated to be 25% (4/16 maternally related individuals), which is lower than 51.4% (18/35) in our family. The higher penetrance found in our family suggested that M7b haplogroup might confer risk for LHON, but this conclusion is insufficient due to small sample sizes. After all, only a very few studies so far focused on haplogroup investigation of LHON cohorts who were harboring the m.14495A>G mutation, with limited data available. Recently, in addition to M haplogroup being reported again as a high-risk factor for LHON, another interesting finding has been noted that in South Indian population, the number of mtDNA mutations is higher in LHON patients than in healthy controls.[33] In the present study, a total of 46 mutations were found in each matrilineal relative (Supplementary Table S1), far exceeding the reported average number of variations in healthy controls (26.23 ± 4.17),[33] further indicating that individual with our mtDNA haplogroup background would become more susceptible to LHON.

It is of interest to note that individual V-5 is unaffected but present a heteroplasmy of 98.45% (Table) and such a high heteroplasmy level can result in an elimination of statistical difference between unaffected carriers and affected (data not shown). We found that she possesses higher mtDNA content as compared with other unaffected mutation carriers. Giordano et al.[34] had put forward the idea that estrogens play a protective role to rescue the viability of LHON cell lines through the activation of mitochondrial biogenesis by using in vitro study approach.[35] And they clearly documented that efficient mitochondrial biogenesis drives incomplete penetrance in LHON.[36] This view is supported by our study in which V-5 as a female carrier had a significantly higher mtDNA amount. But this phenomenon is not limited to female subjects, a male subject who harbors the m.11778G>A mutation at a high-heteroplasmy level, was reported to be unaffected due to high mtDNA copy number.[31] This suggests that the high mtDNA content protecting mutation carriers from LHON is independent of sex. Whether estrogen is still considered to modify the severity of male mitochondrial dysfunction, no relevant studies have been reported so far. But its neuroprotective effect may exist even in male individual.[37,38] It is readily understood that increased mtDNA copy number could compensate mitochondrial dysfunction and therefore impede the development of LHON.[39] According to a mechanism study on mitochondrial energy metabolism, defective mitochondria exhibit strong fusion ability for normal mitochondria and lead to a quick achievement of the energy compensatory.[40] Therefore, high mtDNA copy number means that cell may provide sufficient amount of normal mitochondria to rescue the metabolic damage caused by mutant mtDNA. There is emerging evidence supporting high mtDNA copy number as the protective factor from LHON manifestation,[7,31] although with some controversies.[41,42] Clearly, to increase the cellular mtDNA content would be considered a promising therapeutic strategy for LHON, and a list of compounds have been recommended.[43] But for those who possess 100% mutational load without wild-type mitochondria, whether simply by increasing the number of defective mtDNA also can prevent the expression of LHON may be questionable.[31] We also noted that the penetrance of this family was 18.9% in males (7/37) and 29.7% in females (11/37), respectively, which is different from male prevalence in LHON,[44] suggesting that heteroplasmy level instead of sex is the leading risk factor for carriers with m.14495A>G mutation.

As reported by Bianco et al.,[31] unaffected individuals harboring one of both mutations (m.11778G>A and m.3460G>A) usually possess higher mtDNA content compared with the affected. However, in the current study, carriers versus affected did not reach statistical significance (Supplementary Fig. S3B, *t*-test) in mtDNA content except individual V-5, further indicating heteroplasmy of m.14495A>G rather than

mtDNA content plays a more important part in determining the clinical manifestations of LHON. Based on our result, we propose a modified diagnostic procedure for patient with heteroplasmic mutation, like m.14495A>G. As shown in Supplementary Figure S3C, subjects with mutation loads below 50% would be considered as healthy individuals. Once the observed value is greater than 50%, we need to assess the cellular mtDNA content of the patients. If the blood mtDNA level was below normal value, they would be considered as LHON risk individuals and must have periodical medical check-ups.

In conclusion, this is the first report of m.14495A>G mutation in Asian LHON cohort. We demonstrated that its heteroplasmy level in blood cells can be used as a diagnostic indicator of LHON risk. In addition, this study consolidated the previous finding that higher mtDNA content may protect mutation carriers from LHON even when the heteroplasmy level is high. Overall, these findings provide new insights into the understanding of genesis mechanisms of LHON and also provide valuable suggestion on efficient diagnosis for heteroplasmic patients who might account for an approximately 15% of LHON cohort.[17] Otherwise, we also proved that digital PCR is a promising technology for precise diagnosis of LHON especially in the patients with heteroplasmic mutation.

Acknowledgments

The authors thank the patients and their family members for their generous support, and Jian Gao for help with statistical analysis.

Supported by the Fundamental Research Project of Shenzhen Science and Technology Plan (JCYJ20160429091139605 to BW; JCYJ20180306173215758 to SD).

Disclosure: **S. Li**, None; **S. Duan**, None; **Y. Qin**, None; **S. Lin**, None; **K. Zheng**, None; **X. Li**, None; **L. Zhang**, None; **X. Gu**, None; **K. Yao**, None; **B. Wang**, None

References

1. Dai Y, Wang C, Nie Z, et al. Mutation analysis of Leber's hereditary optic neuropathy using a multi-gene panel. *Biomed Rep*. 2018;8:51–58.
2. Cwerman-Thibault H, Augustin S, Ellouze S, Sahel JA, Corral-Debrinski M. Gene therapy for mitochondrial diseases: Leber hereditary optic neuropathy as the first candidate for a clinical trial. *C R Biol*. 2014;337:193–206.
3. Carelli V, Ross-Cisneros FN, Sadun AA. Mitochondrial dysfunction as a cause of optic neuropathies. *Prog Retin Eye Res*. 2004;23:53–89.
4. Brandon MC, Lott MT, Nguyen KC, et al. MITOMAP: a human mitochondrial genome database–2004 update. *Nucleic Acids Res*. 2005; 33:D611–D613.
5. Mitchell AL, Elson JL, Howell N, Taylor RW, Turnbull DM. Sequence variation in mitochondrial complex I genes: mutation or polymorphism? *J Med Genet*. 2006;43:175–179.
6. Maresca A, Caporali L, Strobbe D, et al. Genetic basis of mitochondrial optic neuropathies. *Curr Mol Med*. 2014;14:985–992.
7. Caporali L, Maresca A, Capristo M, et al. Incomplete penetrance in mitochondrial optic neuropathies. *Mitochondrion*. 2017;36:130–137.
8. Dimitriadis K, Leonhardt M, Yu-Wai-Man P, et al. Leber's hereditary optic neuropathy with late disease onset: clinical and molecular characteristics of 20 patients. *Orphanet J Rare Dis*. 2014;9: 158.
9. Yu-Wai-Man P, Griffiths PG, Brown DT, Howell N, Turnbull DM, Chinnery PF. The epidemiology of Leber hereditary optic neuropathy in the North East of England. *Am J Hum Genet*. 2003; 72:333–339.
10. Hudson G, Carelli V, Spruijt L, et al. Clinical expression of Leber hereditary optic neuropathy is affected by the mitochondrial DNA-haplogroup background. *Am J Hum Genet*. 2007;81: 228–233.
11. Hudson G, Keers S, Yu-Wai-Man P, et al. Identification of an X-chromosomal locus and haplotype modulating the phenotype of a mitochondrial DNA disorder. *Am J Hum Genet*. 2005; 77:1086–1091.
12. Tsao K, Aitken PA, Johns DR. Smoking as an aetiological factor in a pedigree with Leber's hereditary optic neuropathy. *Br J Ophthalmol*. 1999;83:577–581.
13. Kirkman MA, Yu-Wai-Man P, Korsten A, et al. Gene-environment interactions in Leber hereditary optic neuropathy. *Brain*. 2009;132:2317–2326.
14. Giordano L, Deceglie S, d'Adamo P, et al. Cigarette toxicity triggers Leber's hereditary optic neuropathy by affecting mtDNA copy number,

oxidative phosphorylation and ROS detoxification pathways. *Cell Death Dis*. 2015;6:e2021.
15. Torroni A, Petrozzi M, D'Urbano L, et al. Haplotype and phylogenetic analyses suggest that one European-specific mtDNA background plays a role in the expression of Leber hereditary optic neuropathy by increasing the penetrance of the primary mutations 11778 and 14484. *Am J Hum Genet*. 1997;60:1107–1121.
16. Jiang P, Liang M, Zhang C, et al. Biochemical evidence for a mitochondrial genetic modifier in the phenotypic manifestation of Leber's hereditary optic neuropathy-associated mitochondrial DNA mutation. *Hum Mol Genet*. 2016;25:3613–3625.
17. Yu-Wai-Man P, Griffiths PG, Hudson G, Chinnery PF. Inherited mitochondrial optic neuropathies. *J Med Genet*. 2009;46:145–158.
18. Chinnery PF, Andrews RM, Turnbull DM, Howell NN. Leber hereditary optic neuropathy: does heteroplasmy influence the inheritance and expression of the G11778A mitochondrial DNA mutation? *Am J Med Genet*. 2001;98:235–243.
19. Finsterer J, Zarrouk-Mahjoub S. Leber's hereditary optic neuropathy is multiorgan not monoorgan. *Clin Ophthalmol*. 2016;10:2187–2190.
20. Emperador S, Vidal M, Hernandez-Ainsa C, et al. The decrease in mitochondrial DNA mutation load parallels visual recovery in a Leber hereditary optic neuropathy patient. *Front Neurosci*. 2018;12:61.
21. Rieder MJ, Taylor SL, Tobe VO, Nickerson DA. Automating the identification of DNA variations using quality-based fluorescence re-sequencing: analysis of the human mitochondrial genome. *Nucleic Acids Res*. 1998;26:967–973.
22. Howell N, Kubacka I, Xu M, McCullough DA. Leber hereditary optic neuropathy: involvement of the mitochondrial ND1 gene and evidence for an intragenic suppressor mutation. *Am J Hum Genet*. 1991;48:935–942.
23. Pereira L, Soares P, Radivojac P, Li B, Samuels DC. Comparing phylogeny and the predicted pathogenicity of protein variations reveals equal purifying selection across the global human mtDNA diversity. *Am J Hum Genet*. 2011;88:433–439.
24. Song Z, Laleve A, Vallieres C, McGeehan JE, Lloyd RE, Meunier B. Human mitochondrial cytochrome B variants studied in yeast: not all are silent polymorphisms. *Hum Mutat*. 2016;37:933–941.
25. Hofmann S, Jaksch M, Bezold R, et al. Population genetics and disease susceptibility: characterization of central European haplogroups by mtDNA gene mutations, correlation with D loop variants and association with disease. *Hum Mol Genet*. 1997;6:1835–1846.
26. Achilli A, Iommarini L, Olivieri A, et al. Rare primary mitochondrial DNA mutations and probable synergistic variants in Leber's hereditary optic neuropathy. *PLoS One*. 2012;7:e42242.
27. Chinnery PF, Brown DT, Andrews RM, et al. The mitochondrial ND6 gene is a hot spot for mutations that cause Leber's hereditary optic neuropathy. *Brain*. 2001;124:209–218.
28. Urata M, Wada Y, Kim SH, et al. High-sensitivity detection of the A3243G mutation of mitochondrial DNA by a combination of allele-specific PCR and peptide nucleic acid-directed PCR clamping. *Clin Chem*. 2004;50:2045–2051.
29. Genasetti A, Valentino ML, Carelli V, et al. Assessing heteroplasmic load in Leber's hereditary optic neuropathy mutation 3460G->A/MT-ND1 with a real-time PCR quantitative approach. *J Mol Diagn*. 2007;9:538–545.
30. Huoponen K. Leber hereditary optic neuropathy: clinical and molecular genetic findings. *Neurogenetics*. 2001;3:119–125.
31. Bianco A, Bisceglia L, Russo L, et al. High mitochondrial DNA Copy number is a protective factor from vision loss in heteroplasmic Leber's hereditary optic neuropathy (LHON). *Invest Ophthalmol Vis Sci*. 2017;58:2193–2197.
32. Zhang AM, Jia X, Bi R, et al. Mitochondrial DNA haplogroup background affects LHON, but not suspected LHON, in Chinese patients. *PLoS One*. 2011;6:e27750.
33. Saikia BB, Dubey SK, Shanmugam MK, Sundaresan P. Whole mitochondrial genome analysis in South Indian patients with Leber's hereditary optic neuropathy. *Mitochondrion*. 2017;36:21–28.
34. Giordano C, Montopoli M, Perli E, et al. Oestrogens ameliorate mitochondrial dysfunction in Leber's hereditary optic neuropathy. *Brain*. 2011;134:220–234.
35. Pisano A, Preziuso C, Iommarini L, et al. Targeting estrogen receptor beta as preventive therapeutic strategy for Leber's hereditary optic neuropathy. *Hum Mol Genet*. 2015;24:6921–6931.
36. Giordano C, Iommarini L, Giordano L, et al. Efficient mitochondrial biogenesis drives incomplete penetrance in Leber's hereditary optic neuropathy. *Brain*. 2014;137:335–353.
37. Zhou X, Li F, Ge J, et al. Retinal ganglion cell protection by 17-beta-estradiol in a mouse model of inherited glaucoma. *Dev Neurobiol*. 2007;67:603–616.

38. Prokai-Tatrai K, Xin H, Nguyen V, et al. 17beta-estradiol eye drops protect the retinal ganglion cell layer and preserve visual function in an in vivo model of glaucoma. *Mol Pharm*. 2013;10:3253–3261.
39. Wredenberg A, Wibom R, Wilhelmsson H, et al. Increased mitochondrial mass in mitochondrial myopathy mice. *Proc Natl Acad Sci U S A*. 2002;99:15066–15071.
40. Yang L, Long Q, Liu J, et al. Mitochondrial fusion provides an 'initial metabolic complementation' controlled by mtDNA. *Cell Mol Life Sci*. 2015;72:2585–2598.
41. Finsterer J. Do high mtDNA copy numbers truly prevent LHON manifestations? *Invest Ophthalmol Vis Sci*. 2017;58:4076.
42. Finsterer J, Zarrouk-Mahjoub S. Increased mtDNA copy number does not protect against LHON. *Invest Ophthalmol Vis Sci*. 2018;59:330.
43. Ruiz-Pesini E, Emperador S, Lopez-Gallardo E, Hernandez-Ainsa C, Montoya J. Increasing mtDNA levels as therapy for mitochondrial optic neuropathies. *Drug Discov Today*. 2018;23:493–498.
44. Yu-Wai-Man P, Griffiths PG, Chinnery PF. Mitochondrial optic neuropathies - disease mechanisms and therapeutic strategies. *Prog Retin Eye Res*. 2011;30:81–114.